B-SLAM-SIM: A novel approach to evaluate the fusion of Visual SLAM and GPS by example of Direct Sparse Odometry and Blender

Adam Kalisz[1], Florian Particke[1], Dominik Penk[2], Markus Hiller[1] and Jörn Thielecke[1]
[1]*Department of Electrical, Electronic and Communication Engineering, Information Technology (LIKE), Friedrich-Alexander-Universität Erlangen-Nürnberg, Am Wolfsmantel 33, Erlangen, Germany*
[2]*Department of Computer Science, Computer Graphics Lab (LGDV), Friedrich-Alexander-Universität Erlangen-Nürnberg, Cauerstraße 11, Erlangen, Germany*
{*adam.kalisz, florian.particke, dominik.penk, markus.hiller, joern.thielecke*}*@fau.de*

Keywords: Fusion, Global Positioning System, Visual Simultaneous Localization And Mapping, GPS, SLAM, Simulation, Blender

Abstract: In order to account for sensor deficiencies, usually a multi-sensor approach is used where various sensors complement each other. However, synchronization of highly accurate Global Positioning System (GPS) and video measurements requires specialized hardware which is not straightforward to set up. This paper proposes a full simulation environment for data generation and evaluation of Visual Simultaneous Localization and Mapping (Visual SLAM) and GPS based on free and open software. Specifically, image data is created by rendering a virtual environment where camera effects such as Motion Blur and Rolling Shutter can be added. Consequently, a ground truth camera trajectory is available and can be distorted via additive Gaussian noise to understand all parameters involved in the use of fusion algorithms such as the Kalman Filter. The proposed evaluation framework will be published as open source online at https://master.kalisz.co for free use by the research community.

1 INTRODUCTION

Artificial Intelligence and Machine Learning are the main building blocks for many of the recent advances in robotics. Self driving cars usually employ an expensive set of sensors (Sebastian Thrun, Udacity, Inc., 2018) in order to understand their environment. 3D laser scanners are a popular choice for this task. Although such devices can provide highly accurate measurements, they are large, sensitive, cumbersome to transport and need quite some time to create a full scan of the environment. This makes them a great choice to get a metric, real world scale 3D point cloud but hard to operate on moving platforms or vehicles. The area of camera-based localization and mapping is a well-studied field and an impressive amount of work has been done on creating open source algorithms which can easily accomplish this goal. Yet, there are still challenging situations where the addition of a second sensor may be a good option. Some cameras can provide a global reference to where the camera is currently located (geotagging) in video mode, such as recent versions of the GoPro Hero action camera series [1]. It is therefore highly motivating to investigate such cost-effective devices that allow for localization and mapping at the same time. In order to compare fusion of VSLAM and GPS with a ground truth reference, this research is based on a controllable simulation environment where an artist can create challenging scenarios that are not trivial to find in the real world on the one hand and investigate the influence of specific sensor characteristics and deficiencies on the other hand.

2 RELATED WORK

After many years of research in this field, there is already a plethora of sophisticated software packages available which are able to estimate highly accurate camera poses and 3D point clouds from a set of images.

Popular commercial software includes Photoscan (Agisoft LLC, 2014), Reality Capture (Capturing Reality, 2018), built by creators of CMPMVS (Jancosek,

[1]https://gopro.com/compare

Michal and Pajdla, Tomas, 2012) and Syntheyes (Andersson Technologies LLC, 2018).

Although the basic ideas might be similar in all algorithms, they may be distinguished by a few properties. The most obvious difference between todays state-of-the-art approaches may be considered the idea of indirect (feature-based) against direct methods (Krombach et al., 2016). The former transforms image data into a feature space representation first and then proceeds with the camera pose and 3D structure information extraction by minimizing a geometric error. On the contrary, latter methods directly use image data to perform SLAM by minimizing a photometric error, thus those are called direct approaches. Recently, a third approach gains increasing popularity: Machine-Learning methods (Mohanty et al., 2016). Although these could be a game-changer in this research field, up to the authors knowledge all of them either require large datasets specific to a certain scenario used for the mandatory training phase (Vijayanarasimhan et al., 2017) or are only able to reconstruct isolated objects in a scene (Choy et al., 2016). Still, these approaches look very promising (Eslami et al., 2018) and are expected to soon provide mature alternatives to traditional feature extraction and tracking techniques.

Open source software that uses indirect methods includes Blender's (Blender Foundation, 2018) integrated multi view library LibMV (Blender Contributors, 2018), the state-of-the-art of feature-based methods ORB-SLAM2 (Mur-Artal and Tardós, 2017), Visual SfM (Changchang Wu, 2018), COLMAP (Schönberger and Frahm, 2016) and a recent framework called AliceVision, which is funded by the European Union's Horizon 2020 research and innovation programme (Czech Technical University (CTU) et. al., 2018).

Examples of state-of-the-art open source software that uses direct methods is Direct Sparse Odometry (DSO) (Engel et al., 2017), which is used in this work and its predecessor Large Scale Direct SLAM (LSD-SLAM) (Engel et al., 2014). Additionally, hybrid implementations of indirect and direct methods exist, for example Fast Semi-Direct Monocular Visual Odometry (SVO) (Forster et al., 2014).

The fusion of sensors providing a navigation solution and camera-based vision is an active field of research. Related work focused on fusing inertial measurements with visual measurements from a monocular camera (Mourikis and Roumeliotis, 2007), investigated the accurate estimation of a relative bearing between two vehicles by fusing vision algorithms and GPS (Amirloo Abolfathi, 2015) or integrated a custom satellite navigation receiver tightly with a stereo camera (Aumayer, 2016).

To the authors knowledge, however, there is no research which investigates the fusion of direct methods and GPS. During the evaluation of our work, the authors of Direct Sparse Odometry (DSO) published a paper on fusing inertial sensors and Stereo-DSO, calling it Direct Visual-Inertial Odometry (Usenko et al., 2016). However, fusion with GPS still remains an open question. Therefore, this paper aims to propose a flexible pipeline for the research community to evaluate the fusion of GPS and DSO. This includes generation of usually not available ground truth data and the flexibility to investigate various fusion approaches more closely. Our framework targets the influence of sensor deficiencies in special environments which are normally hard to record in an appropriate manner when using real sensors.

3 DATASET

From all the created virtual environments, four of them are included here where qualitative evaluation was performed. Figure 1 depicts their individual trajectories from the top view.

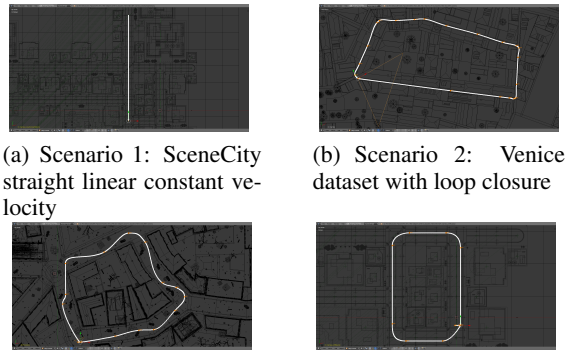

(a) Scenario 1: SceneCity straight linear constant velocity

(b) Scenario 2: Venice dataset with loop closure

(c) Scenario 3: Damaged Downtown dataset with loop closure

(d) Scenario 4: SceneCity dataset with loop closure

Figure 1: Four scenarios have been selected for evaluation

A final render of the scenario visualized in Figure 1(a) is presented in Figure 2(a). Figure 2 includes a few challenging types of sensor characteristics in Visual SLAM applications which can all be simulated using our proposed system. Camera effects such as Motion Blur, Rolling Shutter and Automatic Gain Control (i.e. varying image brightness) can be added. However, the evaluation part of this paper investigates ideal real-time renderings not including any of such errors as we noticed that the DSO algorithm can be quite sensitive to them.

(a) Original (ideal) image

(b) Lens vignetting

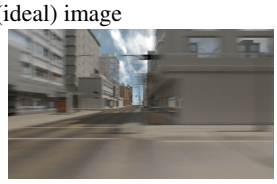

(c) Motion blur

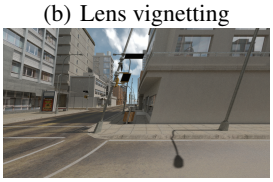

(d) Rolling shutter

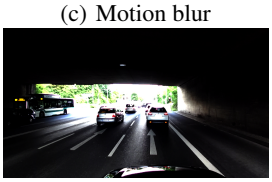

(e) Contre-jour shot

Figure 2: Some of the challenges for Visual SLAM algorithms

The trajectories reconstructed via DSO were usually reasonably good and have been passed on to the processing stage where fusion with GPS was performed. However, we noticed that camera rotations may cause a strong drift. This happened in our experiments more likely in open areas (i.e. wide streets in Scenario 3) as opposed to narrow passageways (such as the camera path through Venice in Scenario 2). Performing two tests where the camera was both rotating and moving on the one hand (compare Figure 3(a)) and only moving while keeping rotation locked on the other hand (compare Figure 3(b)) can clearly show the difference. Figure 3 summarizes the virtual scene and their reconstructions in the DSO.

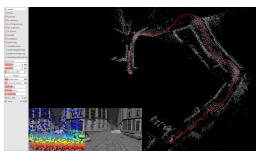

(a) DSO result: Damaged Downtown (rotating camera)

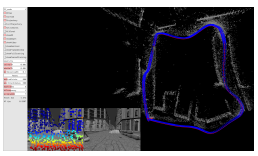

(b) DSO result: Damaged Downtown (no rotating camera)

Figure 3: Virtual environment of a damaged downtown downloaded from the website Open3DModel

4 FUSION

The diversity of available sensors used by robots to sense their environments render multisensor data fusion a challenging task, especially when the measurements of those sensors need to be integrated into a final navigation solution (Mueller and Massaron, 2018).

Multiple sensor readings could be combined in different ways (Khaleghi et al., 2013). Generally, the right approach needs to consider issues like imperfection, modality, dimensionality and correlation of data.

A very elegant and popular way from the class of stochastic fusion methods, that is applicable under Gaussian assumptions, is to use a Kalman filter (Marchthaler and Dingler, 2017).

This chapter provides an overview of the main sensor data fusion concept in this work. Complex integration architectures such as loose, tight and ultra-tight coupling are often employed when sensors are fused. Thus, full access to these sensor sources is required to route back the prediction from a filter step to initialize new calculations. The result is a highly customized system that only works for one type of sensor configuration. In the course of this work, we chose to show capabilities of the proposed framework by evaluating the fusion of DSO and GPS. It is possible, however, to exchange Visual SLAM algorithms freely, as this work examines an uncoupled approach where Visual SLAM and GPS settings can be modified individually in order to investigate their effects.

4.1 Overview

This research is based on the following concept illustrated in Figure 4 which should give the reader an overview of the main components of this work:

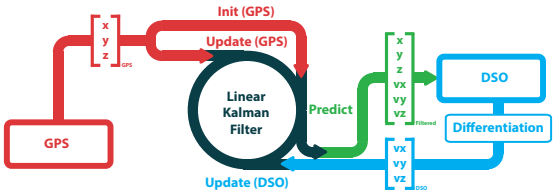

Figure 4: Main filter cycle

A Kalman filter basically consists of a prediction and an update step. The prediction step takes the current state of the system and projects the next state ahead by using the underlying motion model. Additionally, it determines the state covariance matrix and adds uncertainty. The update step will use an available measurement to correct the prediction based on the sensor model. However, since this research fuses

two sensor sources, namely GPS and Visual SLAM, the update step is executed either once or twice, depending on what sensor measurement is available. The Kalman filter algorithm continues recursively by repeating those steps over and over again until all frames are processed or the program ends. Figure 4 depicts this cycle graphically[2]. Firstly, the Kalman filter needs to be initialized. This is done by taking the 3D position provided by the GPS sensor to reduce the delay until the Kalman filter converges to an optimal solution. The Visual SLAM algorithm provides position measurements as well. However, due to unknown transformations of the involved coordinate systems, the use of position updates will lead to wrong results. Therefore, the velocity is calculated via differentiation from the position measurements, which is then used for the update step in the Kalman filter implementation.

At every executed cycle, the Kalman filter provides an estimate of the current state vector, which can then be used to integrate with the sensors through a feedback route using a coupled architecture.

The fusion of GPS measurements with Visual SLAM is prepared using three steps. Firstly, synthetic environments where a virtual camera was moved are generated. This is considered the ground truth reference. Secondly, in order to simulate noisy GPS readings, synthetic noise is added to the ground truth using a Gaussian distribution. Thirdly, the image sequence used in the DSO is generated by means of rendering the viewpoint of the moving camera including any sensor errors (Ehlenbröker et al., 2016) which is then processed by the Visual SLAM algorithm. Finally, the fusion of both Visual SLAM and GPS measurements is performed using a Kalman filter. The remainder of this chapter is dedicated on defining the fusion concept evaluated using our proposed simulation-based framework.

4.2 Coordinate Systems

In order to export properly oriented camera poses from Blender to the DSO algorithm and vice versa, it was necessary to align their coordinate systems. While both are right-handed, they use different up vectors for the orientation of the camera. Blender uses the positive y-axis and DSO uses a negative y-axis as the up vector. However, the urban scenarios in Blender were created in the x-y plane, thus this rotation needs to be taken into account as well.

[2]Please note, that the colors should not mislead the reader in the sense that the prediction and update steps may be disconnected from the main loop. The reason for coloring the components of the cycle like this is to keep the same style throughout this document, especially later in the evaluation plots.

4.3 Linear Kalman Filter

The Kalman filter is a state estimator. Therefore, the physical representation of the camera pose needs to be modeled by first defining a state. The state vector used in this work consists of the position in x, y, z and the respective velocities in v_x, v_y, v_z

$$\mathbf{x}_{\text{Blender}} = \begin{bmatrix} x & v_x & y & v_y & z & v_z \end{bmatrix}^T. \tag{1}$$

The a-priori state $\hat{\mathbf{x}}_k^-$ for timestep k is calculated using a constant velocity motion model (Zhai et al., 2014) and the process noise covariance matrix $\mathbf{Q}_{k-1}$ can be determined by solving the underlying differential equations of the physically based constant velocity motion model (Particke et al., 2017) for the two-dimensional case. For this work a three dimensional extension of the proposed matrix is needed as the state vector supports vertical movements as well and the camera trajectory does not necessarily only consist of planar motion. Based on the proposed power spectral density for velocity σ_v of the physical motion we define the following temporary values

$$\mathrm{d1}_t = \sigma_v \Delta t, \tag{2}$$

$$\mathrm{d2}_t = \sigma_v \frac{\Delta t^2}{2}, \tag{3}$$

and

$$\mathrm{d3}_t = \sigma_v \frac{\Delta t^3}{3} + \mathrm{d1}_t, \tag{4}$$

to compose the process noise as

$$\mathbf{Q}_{k-1} = \begin{bmatrix} \mathrm{d3}_t & \mathrm{d2}_t & 0 & 0 & 0 & 0 \\ \mathrm{d2}_t & \mathrm{d1}_t & 0 & 0 & 0 & 0 \\ 0 & 0 & \mathrm{d3}_t & \mathrm{d2}_t & 0 & 0 \\ 0 & 0 & \mathrm{d2}_t & \mathrm{d1}_t & 0 & 0 \\ 0 & 0 & 0 & 0 & \mathrm{d3}_t & \mathrm{d2}_t \\ 0 & 0 & 0 & 0 & \mathrm{d2}_t & \mathrm{d1}_t \end{bmatrix}_{k-1}. \tag{5}$$

The error model for the simulated GPS in Blender can be trivially provided, since this is a setting that can be comfortably set during the creation of the simulation data. It is much more difficult to determine the error of the DSO and real sensors. However, this work proposes a simulation environment with a user friendly and quick way to investigate specific fusion approaches and how they react on different error models as it offers a full pipeline from importing test data to generating the final plots visualizing positions, velocities and errors of the sensor data fusion with just a few mouse clicks.

5 RESULTS

In order to gain more insight about specific limitations of the investigated fusion algorithm and to show capabilities of the proposed simulation-based framework, the following test cases on each scenario from Figure 1 have been explored:

1. Only position updates from GPS
2. Fusion of position from GPS and DSO
3. Fusion of position from GPS and DSO, where DSO was aligned with ground truth in Blender
4. Fusion of position from GPS and velocity from DSO
5. Variation of GPS frequency from one per frame ($T = 1/25\,\mathrm{s}$) to one per two seconds ($T = 50/25\,\mathrm{s} = 2\,\mathrm{s}$), assuming the video frame rate is set to 25 frames per second.

By default, the initial position in the Kalman filter is set to the zero vector $\begin{bmatrix}0\,\mathrm{m} & 0\,\mathrm{m} & 0\,\mathrm{m}\end{bmatrix}^T$. The standard deviations in the measurement noise covariance matrices for GPS and DSO are set to $\sigma_{\mathrm{GPS}} = 1.0\,\mathrm{m}$ and $\sigma_{\mathrm{DSO}} = 5.0\,\mathrm{m}$, respectively. The frequency of GPS updates is $f_{\mathrm{GPS}} = 25\,\mathrm{Hz}$. The standard deviations of position and velocity used in the state error covariance matrix are $\sigma_{x0} = 0.02\,\mathrm{m}$ and $\sigma_{v0} = 0.4\,\mathrm{m}$, respectively. Finally, the power spectral density used in the process noise covariance matrix is set to $\sigma_v = 0.2\,\mathrm{m}^2/\mathrm{s}^2$. The noisy GPS was simulated with a standard deviation of $\sigma_x = \sigma_y = 1.0\,\mathrm{m}$.

5.1 Scenario 1: SceneCity Constant Linear Velocity

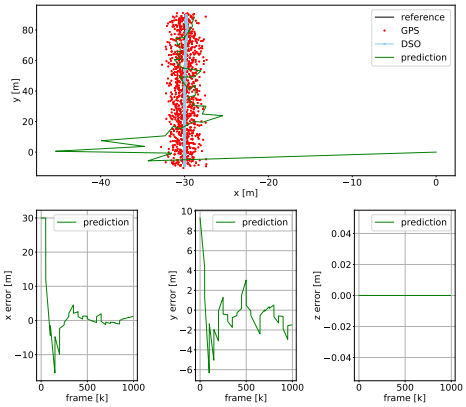

Figure 5: Scenario 1: Only GPS position updates, every 50th frame
Top: 2D trajectory visualizing x and y coordinates
Bottom: RMSE position error of prediction in x, y and z

A basic test case where merely GPS position measurement updates are available every 50th frame is illustrated in Figure 5 showing the standard visualization plots provided by our simulation framework. DSO position measurements, that have been manually aligned with the ground truth in Blender beforehand, are ignored in this case. At every frame a predicted state is calculated using the constant velocity motion model. Therefore, the filtered result contains discontinuities in the position estimate. However, as GPS only updates x and y coordinates, there is no change in z noticeable.

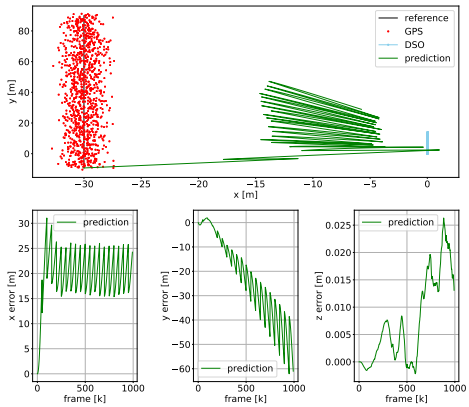

Figure 6: Scenario 1: GPS and DSO position updates, every 50th frame, initialized
Top: 2D trajectory visualizing x and y coordinates
Bottom: RMSE position error of prediction in x, y and z

The fusion of raw GPS and DSO position measurements with an initialization of the Kalman filter using the ground truth is depicted in Figure 6. Due to the more frequent DSO updates the prediction moves very quickly towards the DSO measurements increasing the error in the estimate over time. Our simulation framework helps to identify the presence of a non-zero-mean Gaussian offset in the generated figures of this fusion approach. Hence, raw position measurements are not well suited in this case and thus it is necessary to investigate an alternative fusion method.

Consequently, the fusion of raw GPS position and raw DSO velocity measurement updates is depicted in Figure 7. GPS measurements are taken every 50th frame causing the prediction to converge slower towards the ground truth. However, DSO velocity updates still have an influence on the prediction slowing it down along the y axis. Therefore, even the effects of drift or scale variation can be discovered using our simulation framework.

To summarize, this scenario of a linear camera movement is well suited for the used sensor data fusion approach. Note however, since the DSO is scaled

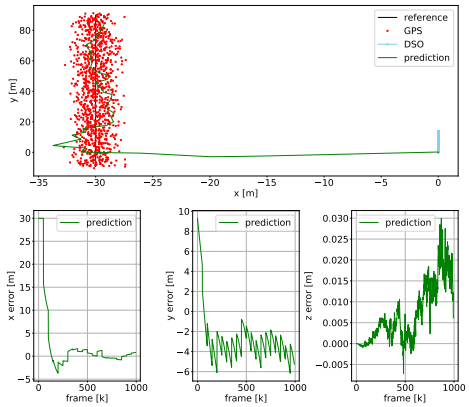

Figure 7: Scenario 1: GPS position and DSO velocity updates, every 50th frame
Top: 2D trajectory visualizing x and y coordinates
Bottom: RMSE position error of prediction in x, y and z

down when compared to the ground truth, velocity updates may slow down the prediction. Consequently, if the DSO has a bigger scale, the prediction may estimate a location ahead of the current one.

5.2 Scenario 2: Venice Loop

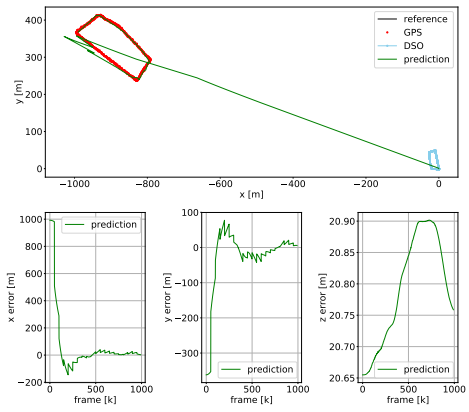

Figure 8: Scenario 2: GPS position and DSO velocity updates, every 50th frame
Top: 2D trajectory visualizing x and y coordinates
Bottom: RMSE position error of prediction in x, y and z

The fusion of raw GPS and raw DSO velocity measurement updates for scenario 2 is presented in Figure 8. GPS readings are provided at every 50th frame. No initialization is provided to the Kalman filter. Although this solution tends to converge for x and y, the frequency of GPS measurement updates is too slow for this scenario causing errors in the estimate most notably when the camera turns.

To summarize, in this scenario consisting of a loop the linear Kalman filter will likely overshoot in parts where the camera turns. This particular scenario consists of very narrow curves and long distances with a mostly linear and straight camera movement. Although the camera did not move very fast around the corners, it can be seen that the introduced nonlinearities had a large influence on the final result.

5.3 Scenario 3: Damaged Downtown Loop

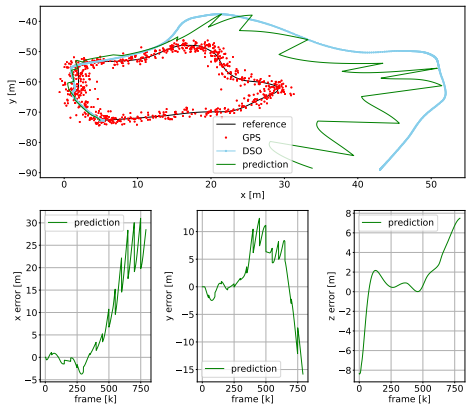

Figure 9: Scenario 3: GPS and DSO (aligned) position updates, every 50th frame, initialized
Top: 2D trajectory visualizing x and y coordinates
Bottom: RMSE position error of prediction in x, y and z

The fusion of raw GPS and aligned DSO position measurement updates for scenario 3 is illustrated in Figure 9. Unfortunately, a proper manual alignment of the DSO trajectory with the ground truth was impossible. At every main corner where the camera is turning, the drift in the DSO trajectory increased dramatically causing it to not close the loop anymore. Consequently, not using any GPS measurements in this situation would never close the loop again. Therefore, GPS readings are provided at every 50th frame. As it is impossible to align the DSO trajectory correctly with the ground truth, this test case will not predict the correct values at all but rather cause them to drift away from the ground truth as was already noticed in Figure 6.

The fusion of raw GPS position and DSO velocity measurement updates is presented in Figure 10. GPS readings are provided at every 50th frame. The slow update rate of GPS causes the prediction to cut corners in this particular scenario which is not desirable for urban environments.

To summarize, this scenario lead to the problem in the DSO, that it did not correctly close the loop. Compared to the GPS measurements, the effects of drift were significant. The evaluations show that a fu-

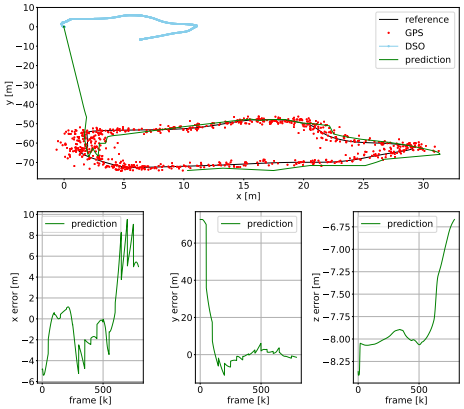

Figure 10: Scenario 3: GPS position and DSO velocity updates, every 50th frame
Top: 2D trajectory visualizing x and y coordinates
Bottom: RMSE position error of prediction in x, y and z

sion with GPS is capable of solving this issue and thus closing the loop, even when the Visual SLAM algorithm does not support it.

5.4 Scenario 4: SceneCity Loop

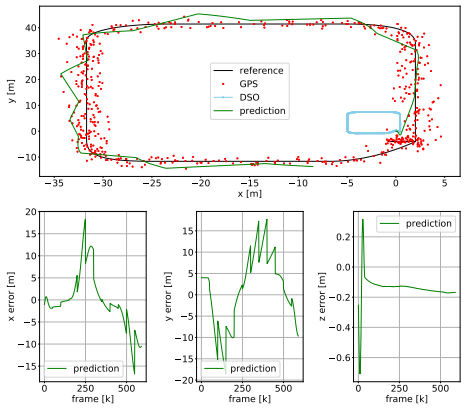

Figure 11: Scenario 4: GPS position and DSO velocity updates, every 50th frame
Top: 2D trajectory visualizing x and y coordinates
Bottom: RMSE position error of prediction in x, y and z

The fusion of raw GPS position and DSO velocity measurement updates for scenario 4 is depicted in Figure 11. GPS readings are provided at every 50th frame. Due to the slow refresh rate of GPS, the predicted trajectory is smoothed, causing it to approximate an ellipse and thus vigorously cut corners. This is not desirable in urban environments.

To summarize, this urban scenario consisting of a loop may cause the linear Kalman filter to overshoot in parts where the camera turns, similar to the Venice dataset. Most notably, each curve did cause the prediction to deviate away a bit more from the true track. Although the corner radius can be considered having a usual size, their non-linear characteristic did still deteriorate the prediction.

6 CONCLUSION

Our approach to simulate sensor data and execute the fusion in Blender provides an attractive way to investigate both the way DSO operates on a diverse set of input images and how this influences sensor data fusion. It was shown that an uncoupled fusion of DSO and GPS offers a promising way to combine these sensors although the current realization is still very basic. There are a few improvements to the system we would like to address in future work. As most realistic problems in robotics involve non-linear functions (Kostas Alexis, University of Nevada, Reno, 2018), the linear Kalman filter is not applicable for these types of motions. An Extended Kalman Filter (EKF) could solve this by using local linearization (Thrun et al., 2005). An alternative may be the use of an Unscented Kalman Filter (UKF) (Wan and Van Der Merwe, 2000) or a Particle Filter (PF) (Rui and Chen, 2001) which could enable a direct comparison of common fusion strategies. Furthermore, the simulation environment could be extended to real cities by generating a virtual city model from imagery of the internet using Structure-from-Motion (SfM) algorithms and GPS trajectories from open map databases enabling researchers to compare the performance of fusion with real and synthetic data at the same time. A detailed evaluation on the effects of sensor errors in Visual SLAM is another interesting topic where subsequent research may continue.

REFERENCES

Agisoft LLC (2014). Agisoft photoscan. Accessed: 2018-07-04.

Amirloo Abolfathi, E. (2015). *Integrating Vision Derived Bearing Measurements with Differential GPS for Vehicle-to-Vehicle Relative Navigation*. PhD thesis, University of Calgary.

Andersson Technologies LLC (2018). Syntheyes. Accessed: 2018-07-04.

Aumayer, B. (2016). Ultra-tightly coupled vision/gnss for automotive applications.

Blender Contributors (2018). Blender foundation: Libmv. Accessed: 2018-07-04.

Blender Foundation (2018). blender.org - home of the blender project - free and open 3d creation software. Accessed: 2018-07-04.

Capturing Reality (2018). Reality capture. Accessed: 2018-07-04.

Changchang Wu (2018). Visualsfm : A visual structure from motion system. Accessed: 2018-07-04.

Choy, C. B., Xu, D., Gwak, J., Chen, K., and Savarese, S. (2016). 3d-r2n2: A unified approach for single and multi-view 3d object reconstruction. In *Proceedings of the European Conference on Computer Vision (ECCV)*.

Czech Technical University (CTU) et. al. (2018). Alice vision: Photogrammetric computer vision framework. Accessed: 2018-07-04.

Ehlenbröker, J.-F., Mönks, U., and Lohweg, V. (2016). Sensor defect detection in multisensor information fusion. *Journal of Sensors and Sensor Systems*, 5(2):337–353.

Engel, J., Koltun, V., and Cremers, D. (2017). Direct sparse odometry. *IEEE transactions on pattern analysis and machine intelligence*, 4.

Engel, J., Schöps, T., and Cremers, D. (2014). Lsd-slam: Large-scale direct monocular slam. In *European Conference on Computer Vision*, pages 834–849. Springer.

Eslami, S. A., Rezende, D. J., Besse, F., Viola, F., Morcos, A. S., Garnelo, M., Ruderman, A., Rusu, A. A., Danihelka, I., Gregor, K., et al. (2018). Neural scene representation and rendering. *Science*, 360(6394):1204–1210.

Forster, C., Pizzoli, M., and Scaramuzza, D. (2014). Svo: Fast semi-direct monocular visual odometry. In *Robotics and Automation (ICRA), 2014 IEEE International Conference on*, pages 15–22. IEEE.

Jancosek, Michal and Pajdla, Tomas (2012). Cmp sfm web service. Accessed: 2018-07-04.

Khaleghi, B., Khamis, A., Karray, F., and Razavi, S. (2013). Multisensor data fusion: A review of the state-of-the-art. 14.

Kostas Alexis, University of Nevada, Reno (2018). Lecture slides - dr. kostas alexis. Accessed: 2018-07-08.

Krombach, N., Droeschel, D., and Behnke, S. (2016). Combining feature-based and direct methods for semi-dense real-time stereo visual odometry. In *International Conference on Intelligent Autonomous Systems*, pages 855–868. Springer.

Marchthaler, R. and Dingler, S. (2017). *Kalman-Filter: Einführung in die Zustandsschätzung und ihre Anwendung für eingebettete Systeme*. SpringerLink : Bücher. Springer Fachmedien Wiesbaden.

Mohanty, V., Agrawal, S., Datta, S., Ghosh, A., Sharma, V. D., and Chakravarty, D. (2016). Deepvo: A deep learning approach for monocular visual odometry. *CoRR*, abs/1611.06069.

Mourikis, A. I. and Roumeliotis, S. I. (2007). A multi-state constraint kalman filter for vision-aided inertial navigation. In *in Proc. IEEE Int. Conf. on Robotics and Automation*, pages 10–14.

Mueller, J. and Massaron, L. (2018). *Artificial Intelligence For Dummies*. Wiley.

Mur-Artal, R. and Tardós, J. D. (2017). Orb-slam2: An open-source slam system for monocular, stereo, and rgb-d cameras. *IEEE Transactions on Robotics*, 33(5):1255–1262.

Particke, Hiller, Patino-Studencki, Sippl, Feist, and Thielecke (2017). Multiple intention tracking by a generalized potential field approach.

Rui, Y. and Chen, Y. (2001). Better proposal distributions: Object tracking using unscented particle filter. In *Computer Vision and Pattern Recognition, 2001. CVPR 2001. Proceedings of the 2001 IEEE Computer Society Conference on*, volume 2, pages II–II. IEEE.

Schönberger, J. L. and Frahm, J.-M. (2016). Structure-from-motion revisited. In *Conference on Computer Vision and Pattern Recognition (CVPR)*.

Sebastian Thrun, Udacity, Inc. (2018). Artificial intelligence for robotics. Accessed: 2018-07-04.

Thrun, S., Burgard, W., and Fox, D. (2005). *Probabilistic Robotics (Intelligent Robotics and Autonomous Agents)*. The MIT Press.

Usenko, V., Engel, J., Stückler, J., and Cremers, D. (2016). Direct visual-inertial odometry with stereo cameras. In *Robotics and Automation (ICRA), 2016 IEEE International Conference on*, pages 1885–1892. IEEE.

Vijayanarasimhan, S., Ricco, S., Schmid, C., Sukthankar, R., and Fragkiadaki, K. (2017). Sfm-net: Learning of structure and motion from video. *CoRR*, abs/1704.07804.

Wan, E. and Van Der Merwe, R. (2000). The unscented kalman filter for nonlinear estimation. pages 153–158.

Zhai, G., Meng, H., and Wang, X. (2014). A constant speed changing rate and constant turn rate model for maneuvering target tracking. *Sensors*, 14(3):5239–5253.